PANTELIDES, S. T., MICKISH, D. J. & KUNZ, A. B. (1974). *Phys. Rev. B*, **10**, 5203-5212.
PATTISON, P. & WEYRICH, W. (1979). *J. Phys. Chem. Solids*, **40**, 213-222.
PODLOUCKY, R. & REDINGER, J. (1984). *J. Phys. C*, **16**, 6955-6969.
REDINGER, J. & SCHWARZ, K. (1981). *Z. Phys. B*, **40**, 269-276.
SCHÜLKE, W. (1977). *Phys. Status Solidi B*, **82**, 229-235.
SCHWARZ, K. & SCHULZ, H. (1978). *Acta Cryst.* A**34**, 994-999.
TONG, B. Y. & LAM, L. (1978). *Phys. Rev. A*, **18**, 552-558.
WATSON, R. E. (1958). *Phys. Rev.* **111**, 1108-1110.
WILLIAMS, B. G. (1977). Editor. *Compton Scattering*. London: McGraw-Hill.

Acta Cryst. (1989). A**45**, 485-490

New Surface Patches for Minimal Balance Surfaces. III. Infinite Strips

By WERNER FISCHER AND ELKE KOCH

Institut für Mineralogie der Universität Marburg, Hans-Meerwein-Strasse, D-3550 Marburg, Federal Republic of Germany

(*Received* 1 *December* 1988; *accepted* 7 *March* 1989)

Abstract

Two new families of minimal balance surfaces are described. Their surface patches are not finite but have the shape of infinite strips. Such a strip is bounded by two congruent zigzag lines in one case or by a zigzag line and a meander line in the other case. In addition, certain minimal balance surfaces derived before with the aid of finite surface patches can also be generated from infinite strip-like surface patches.

1. Introduction

A minimal balance surface subdivides R^3 into two disjunct congruent and multiply connected labyrinths (Fischer & Koch, 1987). With one exception, the Y^* or gyroid surface (*cf.* Schoen, 1970; Fischer & Koch, 1987), all minimal balance surfaces known to the authors contain a so-called linear skeletal net, *i.e.* a set of twofold axes totally embedded within the surface.

On the other hand, an appropriate set of twofold axes, *i.e.* a set of twofold axes defined by a group-subgroup pair of space groups with index 2, may be used as generating linear net for one or several minimal balance surfaces. All conceivable sets of such twofold axes have been tabulated before (Koch & Fischer, 1988).

If all twofold axes within such a set are three-dimensionally connected, in general skew circuits may be found that may be spanned disc-like by a patch of a minimal surface. The families of such minimal balance surfaces have been derived completely (Fischer & Koch, 1987; Koch & Fischer, 1988).

So far, three kinds of surface patches have been described for sets of twofold axes disintegrating into parallel flat nets: catenoids (Koch & Fischer, 1988), branched catenoids (Fischer & Koch, 1989), and multiple catenoids (Koch & Fischer, 1989). Each such surface patch is spanned by two flat polygons as generating circuits. These polygons may be either convex or concave with one point of self-contact.

In addition, a fourth kind of surface patch is compatible with parallel flat nets of twofold axes, namely strips of infinite length. Instead of two polygons such a strip is bounded by two infinite zigzag or meander lines which play a role analogous to that of the generating circuits of finite surface patches.

2. Strip-like surface patches

Strip-like surface patches are compatible exclusively with those sets of twofold axes which consist of parallel square or rectangular nets [cases 24, 26, 27, 29, 30 and 32 in Table 1 of Koch & Fischer (1988)]. As one direction parallel to the nets is necessarily distinguished as the infinite direction of the strips, only twofold rotation axes perpendicular to the nets are compatible with strip-like surface patches. Three-, four- and sixfold rotation axes would necessarily give rise to intersection of the strips and, therefore, to self-intersection of the generated minimal surface.

Each strip is bounded by a first zigzag or meander line formed within one quadrangular net and a second such line from a neighbouring net. With respect to the underlying quadrangular nets zigzag lines run in diagonal directions whereas meander lines extend parallel to the twofold axes forming the nets. The two boundary lines of a strip-like surface patch must run parallel and their middle lines must be located directly above each other.

In this way strips of seven different kinds may be constructed. For five kinds the shape of the strips is such that additional twofold axes occur which are embedded within the strips. As a consequence, the linear skeletal net of a minimal balance surface built

0108-7673/89/070485-06$03.00

Table 1. *Minimal balance surfaces of previously known families generated by strip-like surface patches*

Minimal balance surface	Group-subgroup pair G–H	Strips: Direction	Strips: Symmetry G_r–H_r	Number of surfaces
CLP	$P4_2/mmc$-$Pmmm$	⟨100⟩	$P(m2)m$-$P(m2)m$	2
	$P4_2/nbc$-$P\bar{4}2c$	⟨100⟩	$P(12/c)1$-$P(12)1$	2
	$P4_2/mbc$-$P4_2/m$	⟨100⟩	$P(mc)2_1$-$P(m1)1$	2
	$P4_2/nmc$-$P4_2mc$	⟨100⟩	$P(11)2_1/m$-$P(11)m$	2
	$P4_222$-$P222$	⟨100⟩	$P(12)1$-$P(12)1$	2
	$P4_22_12$-$P4_2$	⟨100⟩	$P(11)2_1$-$P(11)1$	2
	$P\bar{4}m2$-$Pmm2$	⟨100⟩	$P(11)m$-$P(11)m$	2
	$P\bar{4}b2$-$P\bar{4}$	⟨100⟩	$P(1c)1$-$P(11)1$	2
	$P4_2/mcm$-$Cmmm$	⟨110⟩	$P(m2)m$-$P(m2)m$	2
	$P4_2/nnm$-$Cmma$	⟨110⟩	$P(c2)m$-$P(c2)m$	2
	$P4_222$-$C222$	⟨110⟩	$P(12)1$-$P(12)1$	2
	$P\bar{4}2m$-$Cmm2$	⟨110⟩	$P(11)m$-$P(11)m$	2
oCLP	$Cccm$-$P112/m$	⟨110⟩	$P(m1)1$-$P(m1)1$	2
	$Ccca$-$Ccc2$	⟨110⟩	$P(\bar{1}\bar{1})\bar{1}$-$P(11)1$	2
	$C222$-$P112$	⟨110⟩	$P(11)1$-$P(11)1$	2
	$Pnnn$-$P12/n1$	⟨101⟩	$P(c1)1$-$P(c1)1$	2
	$Pban$-$Pb2n$	⟨101⟩	$P(\bar{1}\bar{1})\bar{1}$-$P(11)1$	2
	$Pccm$-$P112/m$	⟨110⟩	$P(m1)1$-$P(m1)1$	2
	$P222$-$P121$	⟨101⟩	$P(11)1$-$P(11)1$	2
tD	$I4_1/amd$-$I4_1md$	⟨100⟩	$P(11)2/m$-$P(11)m$	1
	$I4_1/acd$-$I4_1/a$	⟨100⟩	$P(cc)2$-$P(c1)1$	1
	$I4_122$-$I4_1$	⟨100⟩	$P(11)2$-$P(11)1$	1
	$I4_1/amd$-$Imma$	⟨100⟩	$P(c2)m$-$P(c2)m$	1
	$I4_1/acd$-$I\bar{4}2d$	⟨100⟩	$P(12/c)1$-$P(12)1$	1
	$I4_122$-$I2_12_12_1$	⟨100⟩	$P(12)1$-$P(12)1$	1
	$I\bar{4}m2$-$Imm2$	⟨100⟩	$P(11)m$-$P(11)m$	2
	$I\bar{4}c2$-$I\bar{4}$	⟨100⟩	$P(1c)1$-$P(11)1$	2
oDa	$Fddd$-$Fdd2$	⟨110⟩	$P(\bar{1}\bar{1})\bar{1}$-$P(11)1$	1
	$Fddd$-$C12/c1$	⟨101⟩	$P(c1)1$-$P(c1)1$	1
	$F222$-$C121$	⟨101⟩	$P(11)1$-$P(11)1$	2
oDb	$Ccca$-$Pnna$	[010]	$P(12/c)1$-$P(12)1$	2
	$Ibam$-$Ib2m$	[001]	$P(11)2_1/m$-$P(11)m$	2
	$Cmma$-$Pmma$	[100]	$P(m2)m$-$P(m2)m$	2
	$C222$-$P2_122$	[010]	$P(12)1$-$P(12)1$	2
	$Pban$-$Pb2n$	[001]	$P(\bar{1}\bar{1})\bar{1}$-$P(11)1$	2
	$Pccm$-$Pc2m$	[001]	$P(11)m$-$P(11)m$	2
	$Ibam$-$I112/m$	[010], [100]	$P(mc)2_1$-$P(m1)1$	4
	$I222$-$I121$	[100], [001]	$P(11)2_1$-$P(11)1$	4
	$Pban$-$P112/n$	[100], [010]	$P(1c)1$-$P(11)1$	4
	$Pccm$-$P112/m$	[100], [010]	$P(m1)1$-$P(m1)1$	4
	$P222$-$P121$	[100], [001]	$P(11)1$-$P(11)1$	4

up from such strips is more comprehensive than the generating linear net that has been used. Therefore, the resulting minimal surface may also be generated by disc-like surface patches, and it belongs to one of the known families. Only two kinds of strips, the most complicated ones, give rise to new families of minimal balance surfaces.

3. Previously known minimal balance surfaces generated by strip-like surface patches

Information on all minimal balance surfaces which may be generated from disk-like as well as from strip-like surface patches is gathered in Table 1. The respective families of minimal surfaces are symbolized in column 1 (*cf.* Koch & Fischer, 1988). All group–subgroup pairs G–H compatible with a given kind of strip-like surface patches are tabulated in column 2. The direction of the strips - referred to a conventional basis of G - is indicated in column 3. The strip symmetry is described (column 4) by a group-subgroup pair G_r–H_r of rod groups with $G_r \subset G$ and $H_r \subset H$. The index of H_r in G_r may be either 2 or 1. In the latter case no symmetry operations of G exist that interchange the two sides of a strip and, therefore, G_r and H_r coincide. The rod groups are symbolized according to Bohm & Dornberger-Schiff (1967). In addition, the following rules are observed: (1) The infinite direction of the strips is chosen to be the **c** direction in the rod-group symbol. (2) The **b** direction of the symbol is chosen perpendicular to **c** and parallel to the plane nets of twofold axes. Consequently, the **a** direction must run perpendicular to the plane nets. The number of equivalent surfaces that may be generated within a set of twofold axes is displayed in the last column.

CLP and oCLP surfaces

Case 24 of Table 1 of Koch & Fischer (1988) refers to square nets of twofold axes stacked directly upon each other. Such nets allow strip-like surface patches bounded by two congruent zigzag lines (*cf.* Fig. 1). The corresponding minimal balance surfaces belong to the tetragonal family *CLP*. All strips of the same layer of a *CLP* surface, *i.e.* all strips spanned between the same two square nets, run parallel whereas strips of neighbouring layers are oriented perpendicular to each other. As there exist two possibilities to choose the strip direction in the first layer each set of square nets allows two congruent *CLP* surfaces.

Case 24 refers to 46 types of group-subgroup pairs in total [*cf.* Koch & Fischer (1988), Table 1], 12 of which are compatible with strip-like surface patches as described above. As the inherent symmetry of a *CLP* surface is $P4_2/mcm$-$P4_2/mmc$ there exists no natural summit under the pairs G-H listed in Table 1. The subgroup index of the pairs G-H with respect to the inherent symmetry is 2 for the upper four pairs, 4 for the next six pairs, and 8 for the last two pairs. For all 12 types the intersection group $N_E(G) \cap N_E(H)$ of the Euclidean normalizers of G and H maps the two congruent *CLP* surfaces onto another.

The inherent symmetry of a corresponding strip, $P(mc)m$-$P(m2)m$, also does not occur in Table 1. All listed pairs G_r-H_r are subgroups of the inherent symmetry and all these pairs differ. The fictitious double occurrence of some of them, *e.g.* of $P(m2)m$-$P(m2)m$, results from a doubling of the translation period for the second pair which cannot be made evident by the symbols.

The orthorhombic analogue of case 24 is case 26, *i.e.* rectangular nets stacked directly upon each other. Again zigzag strips may be formed. The corresponding minimal surfaces belong to the family *oCLP*.* Seven out of 33 types of space-group pairs referring to case 26 are compatible with *oCLP* surfaces. The first two pairs listed in Table 1 are subgroups of index 2 of the inherent symmetry $Pccm$-$Cccm$ of *oCLP* surfaces; the index is 4 for the next four pairs and 8 for the last pair. The inherent symmetry of the strips is $P(2/m1)1$-$P(m1)1$.

tD and *oDa* surfaces

Congruent parallel square nets of twofold axes may be stacked in such a way that all vertices of a first net are located between the polygon centres of the two neighbouring nets. Such sets of twofold axes belong to case 29. Again strips may be spanned between two congruent parallel zigzag lines from two adjacent nets (*cf.* Fig. 2). The minimal balance surfaces generated by such strips belong to family *tD*. As for *CLP* surfaces, all strips of one layer run parallel whereas strips of neighbouring layers are perpendicular to each other. Therefore, each such set of twofold axes is compatible with two congruent *tD* surfaces.

The inherent symmetry of a *tD* surface is $P4_2/nnm$-$I4_1/amd$, that of a corresponding strip is $P(cc)m$-$P(c2)m$. Case 29 refers to seven types of group-subgroup pairs, five of which are compatible with *tD* surfaces. Two of these five, namely $I\bar{4}m2$-$Imm2$ and $I\bar{4}c2$-$I\bar{4}$, allow both congruent *tD* surfaces. The other three are consistent with one *tD* surface only. In the case of $I4_1/acd$-$I\bar{4}2d$ the inversion centres must lie on the surface, a condition that can be fulfilled by only one of the two surfaces. In the case of $I4_1/amd$-$Imma$ and $I4_122$-$I2_12_12_1$ the twofold axes .2. contained in G as well as in H must not coincide with the central axes of the strips but run perpendicular to the strips.

The first three group-subgroup pairs listed in Table 1 belong to case 39 instead of case 29. The corresponding sets of twofold axes contain, in addition to the square nets, sets of isolated twofold axes parallel to the plane nets. As a twofold axis in the infinite direction of a strip belongs to its inherent symmetry the additional twofold axes of case 39 play a similar role to the inversion centres for $I4_1/acd$-$I\bar{4}2d$. There exists, of course, a second possibility of handling case 39 and the *tD* surfaces: instead of strips bounded by two zigzag lines and having a twofold axis as middle line one may regard more slender strips with one zigzag line and one straight line as boundaries.

Case 30, the orthorhombic analogue of case 29, refers to sets of rectangular nets with a corresponding stacking sequence. The respective strips generate the orthorhombic family of minimal surfaces *oDa* with inherent symmetry $Pnnn$-$Fddd$. Again each set of rectangular nets spans two congruent *oDa* surfaces, but merely space-group pairs of type $F222$-$C121$ are compatible with both surfaces. For $Fddd$-$Fdd2$ the

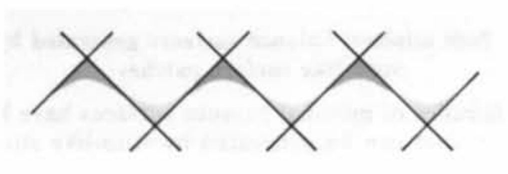

Fig. 1. Strip-like surface patch generating a *CLP* surface.

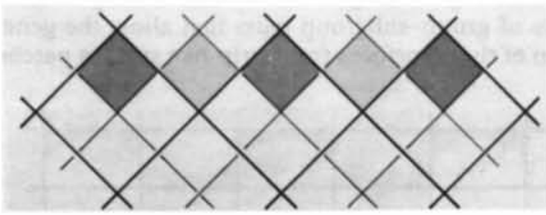

Fig. 2. Strip-like surface patch generating a *tD* surface.

* The symmetry considerations for *oCLP* surfaces have revealed the omission of one possibility for the generation of *oCLP* surfaces from disc-like surface patches in Table 1 of Koch & Fischer (1988): *oCLP* surfaces may be generated from skew 8-gons with chair form spanned by sets of twofold axes belonging to case 16. The corresponding space-group pairs are: $Pban$-$Pnan(2c)$, $Pccm$-$Pncm(2b)$, $P222$-$P222_1(2c)$.

inversion centres of *Fddd* have to lie on the surface, whereas for *Fddd*–*C*12/*c*1 the inversion centres are forbidden to lie on the surface. The inherent strip symmetry of *oDa* surfaces is *P*(2/*c*1)1–*P*(*c*1)1.

oDb surfaces

The sets of rectangular nets belonging to case 26 allow – in addition to the zigzag strips described above – strips bounded by two congruent meander lines and running parallel to the twofold axes of the nets (*cf.* Fig. 3). The resulting minimal surfaces belong to the orthorhombic family *oDb* with inherent symmetry *Cmma*–*Imma*. As all strips of an *oDb* surface are parallel to each other a specialization of the orthorhombic nets to square nets does not enhance the symmetry of the generated surface. The inherent strip symmetry is *P*(*mc*)*m*–*P*(*m*2)*m*.

In principle, each set of rectangular nets enables two pairs of congruent *oDb* surfaces. The strips of congruent surfaces run parallel, those of noncongruent surfaces are perpendicular to each other.

Eleven types of group–subgroup pairs are compatible with *oDb* surfaces. The first six of them allow only one strip direction (*cf.* Table 1, column 3), *i.e.* only two congruent surfaces. This may be understood from the following symmetry arguments: Additional twofold axes ..2 parallel to the nets must not run parallel to the strips (*Ccca*–*Pnna*, $C222$–$P2_122$). Inversion centres on the surfaces are compatible with one strip direction only (*Ibam*–*Ib*2*m*, *Pban*–*Pb*2*n*). Mirror planes perpendicular to the rectangular nets must necessarily be perpendicular to the strip direction (*Cmma*–*Pmma*, *Pccm*–*Pc*2*m*). In all these cases the affine normalizer of *H* is orthorhombic and, therefore, the **a** and **b** directions play different roles with respect to *G*–*H*. In contrast, the affine normalizers of *G* and *H* are at least tetragonal for the last five pairs and, as a consequence, four *oDb* surfaces may be generated.

4. New minimal balance surfaces generated by strip-like surface patches

Two families of minimal balance surfaces have been derived, that can be generated by strip-like surface patches but not by smaller ones bounded by twofold axes. Table 2 displays information on these surfaces. Column 1 gives a symbol, column 2 the genus. All types of group–subgroup pairs that allow the generation of these surfaces from strip-like surface patches

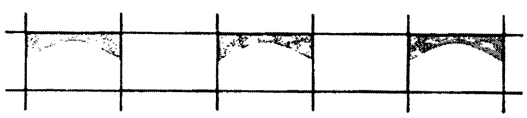

Fig. 3. Strip-like surface patch generating an *oDb* surface.

are listed in column 3, the first one showing the inherent symmetry of the surfaces. The next three columns display information on the strips: the strip direction, the rod-group symmetry, and some coordinate triplets describing the two boundaries of a strip. The last column gives the number of surfaces of this type that may be generated within the same set of twofold axes.

*Minimal balance surfaces ST*1

Special rectangular nets of twofold axes with edge-length ratio $1:3^{1/2}$ may be stacked in a hexagonal sequence with neighbouring nets rotated against each other by 60° [case 27 in Table 1 of Koch & Fischer (1988)]. Then each pair of adjacent nets coincides in the direction of one of their diagonals. The corresonding zigzag lines in this direction span strip-like surface patches which give rise to minimal balance surfaces of a new family, designated *ST*1 (Figs. 4 and 5).

All strips of such a minimal surface bounded by the same two rectangular nets run parallel, but neighbouring strips differ in their orientation. Strips from adjacent layers run in directions rotated by 60° against each other. Each set of nets referring to case 27 is compatible with one *ST*1 surface only.

The inherent symmetry $P6_222$–$P6_422(2c)$ of *ST*1 surfaces coincides with the inherent symmetry of *HS*3 surfaces (*cf.* Koch & Fischer, 1988). Therefore, each *ST*1 surface is complementary to one *HS*3 surface. The translation period perpendicular to the nets of twofold axes comprehends three layers with respect to $P6_222$, but six layers with respect to $P6_422(2c)$.

*Minimal balance surfaces ST*2

Parallel square nets of different size and orientation form the sets of twofold axes belonging to case 32. Zigzag lines within the wider nets and meander lines within the nets with the smaller squares coincide in their directions. Therefore, strips may be spanned between a zigzag line and a meander line from adjacent nets (Fig. 6). They generate minimal balance surfaces of a second new family, named *ST*2 (Fig. 7).

All strips from the same layer of an *ST*2 surface run parallel, but the orientation of neighbouring strips is different. Strips of adjacent layers run parallel, too, if the corresponding common net is formed by the small squares. They run perpendicular to each other, if the layers have one of the wider nets in common.

The inherent symmetry of an *ST*2 surface is $P4_2/nbc$–$P4_2/n$. A translation period perpendicular to the square nets, *i.e.* parallel to **c**, comprehends four layers of strips, with respect to $P4_2/nbc$ as well as with regard to $P4_2/n$. In addition *ST*2 surfaces may be generated with symmetry $P4_222$–$P4_2$. The other two types of space-group pairs belonging to case 32 are incompatible with *ST*2 surfaces.

Table 2. *New minimal balance surfaces generated by strip-like surface patches*

Minimal balance surface	Genus	Group–subgroup pair	Strips: Direction	Strips: Symmetry	Strips: Coordinates	Number of equivalent surfaces
*ST*1	7	$P6_222$–$P6_422(2c)$	⟨010⟩	$P(12)1$–$P(12)1$	$\ldots, 00\frac{1}{6}, 1\frac{1}{2}\frac{1}{6}, 10\frac{1}{6}, \ldots/$	1
		$P6_422$–$P6_4$	⟨010⟩	$P(11)1$–$P(11)1$	$\ldots, 00\frac{\bar{1}}{6}, \frac{1}{2}\frac{1}{2}\frac{\bar{1}}{6}, 10\frac{\bar{1}}{6}, \ldots$	
*ST*2	7	$P4_2/nbc$–$P4_2/n$	⟨100⟩	$P(1c)1$–$P(11)1$	$\ldots, 0\frac{1}{2}\frac{1}{4}, 00\frac{1}{4}, \frac{1}{2}0\frac{1}{4}, \frac{1}{2}\frac{1}{2}\frac{1}{4}, 1\frac{1}{2}\frac{1}{4}, \ldots/$	4
		$P4_222$–$P4_2$	⟨100⟩	$P(11)1$–$P(11)1$	$\ldots, 0\frac{1}{2}0, \frac{1}{2}00, 1\frac{1}{2}0, \ldots$	

As may be learned from Fig. 6 an arbitrarily chosen first zigzag line may be combined with two different meander lines out of each of the adjacent nets.

Therefore, four different *ST*2 surfaces may be generated within each set of twofold axes belonging to case 32. These four surfaces are congruent and complementary. They can be mapped onto each other by the intersection group

$$N_E(P4_2/nbc) \cap N_E(P4_2/n) = P4/mmm\left(\frac{a-b}{2}, \frac{a+b}{2}, \frac{c}{2}\right).$$

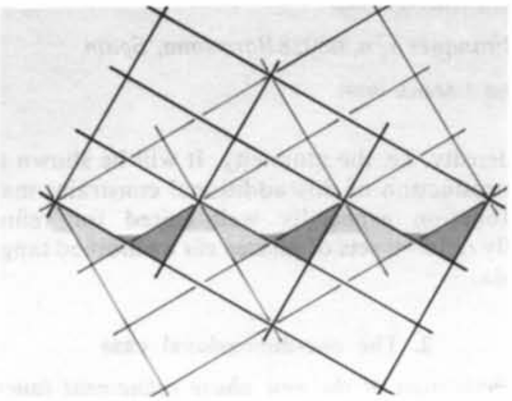

Fig. 4. Strip-like surface patch generating a minimal surface *ST*1 with symmetry $P6_222$–$P6_422(2c)$.

In addition, these four surfaces are complementary to four *BC*2 surfaces (*cf.* Fischer & Koch, 1989) with inherent symmetry $P4_2/nnm$–$P4_2nm$. The genus is 7 for *ST*2 surfaces as well as for *BC*2 surfaces.

5. Common properties of *ST* surfaces

As multiple catenoids may be regarded as resulting from fusion of *n* neighbouring catenoids, strip-like surface patches may be imagined as resulting from fusion of an entire row of infinitely many catenoids or branched catenoids. The fusion of one row of catenoids produces two strip-like surface patches.

New minimal balance surfaces are generated only by strips of which the inherent symmetry does not contain symmetry operations that interchange the two

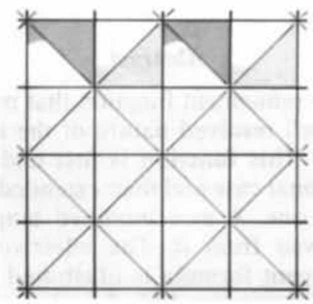

Fig. 6. Strip-like surface patch generating a minimal surface *ST*2 with symmetry $P4_2/nbc$–$P4_2/n$.

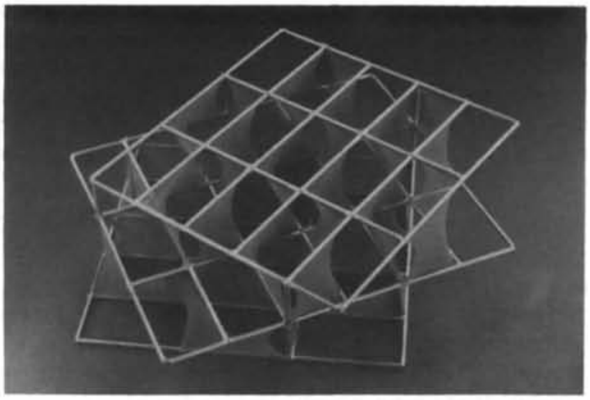

Fig. 5. Model of a minimal surface *ST*1 with symmetry $P6_222$–$P6_422(2c)$.

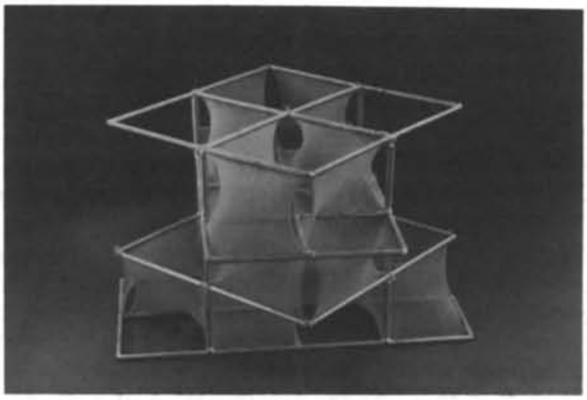

Fig. 7. Model of a minimal surface *ST*2 with symmetry $P4_2/nbc$–$P4_2/n$.

sides of a strip. As a consequence, the new surfaces form two different kinds of channels parallel to the strips, whereas the *CLP*, *oCLP*, *tD*, *oDa* and *oDb* surfaces form only one kind each.

In contrast to minimal balance surfaces generated from catenoids, branched catenoids and multiple catenoids, minimal surfaces that may be generated from strip-like surface patches seem not to be restricted with respect to the axial ratio c/a. Apparently the distance between the rectangular nets may grow arbitrarily large. This property is not surprising with respect to those minimal surfaces that may be generated also from disc-like surface patches. With respect to *ST*1 and *ST*2 surfaces the following idea may be helpful: a strip-like surface patch approximates in its central part more and more to a plane if the distance between its two boundaries becomes wider and wider.

References

BOHM, J. & DORNBERGER-SCHIFF, K. (1967). *Acta Cryst.* **23**, 913-933.
FISCHER, W. & KOCH, E. (1987). *Z. Kristallogr.* **179**, 31-52.
FISCHER, W. & KOCH, E. (1989). *Acta Cryst.* **A45**, 166-169.
KOCH, E. & FISCHER, W. (1988). *Z. Kristallogr.* **183**, 129-152.
KOCH, E. & FISCHER, W. (1989). *Acta Cryst.* **A45**, 169-174.
SCHOEN, A. H. (1970). *Infinite Periodic Minimal Surfaces Without Self-Intersections.* NASA Tech. Note No. D-5541.

Acta Cryst. (1989). A**45**, 490-494

A Geometrically Constrained Phase Refinement Function: the Derivation of a New Modified Tangent Formula

BY JORDI RIUS AND CARLES MIRAVITLLES

Institut de Ciència de Materials (CSIC), c/Martí-Franquès s/n, 08028 *Barcelona, Spain*

(*Received* 14 *December* 1988; *accepted* 7 *March* 1989)

Abstract

A new phase refinement function that makes explicit use of the well resolved nature of the atomic peaks is presented. This function is first deduced for the one-dimensional case and then extended to the three-dimensional one. A new modified tangent formula can be derived from it. The effectiveness of this modified tangent formula is illustrated on the basis of some test structures. This function also seems to provide the *XMY* function of Debaerdemaeker & Woolfson [*Acta Cryst.* (1983), A39, 193-196] with a possible rational explanation.

1. Introduction

As a logical consequence of the availability of faster computers, a number of new multisolution direct methods have been developed in the last years for refining initially random sets of phases, *e.g.* the *YZARC* method of Baggio, Woolfson, Declercq & Germain (1978), the *RANTAN* approach of Yao Jia-xing (1981), the *XMY* function of Debaerdemaeker & Woolfson (1983) and more recently the Sayre (1952) equation tangent formula discussed by Debaerdemaeker, Tate & Woolfson (1985, 1988). Following this trend, a new method has been investigated. It is based on the maximization of a function that explicitly incorporates, besides the positivity, another general and important property of the electron density, *i.e.* the atomicity. It will be shown that the introduction of this additional constraint makes this function especially well suited for refining initially random sets of phases *via* a modified tangent formula.

2. The one-dimensional case

2.1. *Derivation of the new phase refinement function*

As is well known (Cochran, 1952), the integral

$$a^2 \int_\alpha \rho^3(r)\,\mathrm{d}r \qquad (1)$$

must be a strong maximum, since $\rho(r)$, *i.e.* the electron density distribution of a one-dimensional model structure of cell period a, is positive and principally located at the atomic positions. On the other hand, if t represents a shift approximately equal to the average width of the atomic peaks, and since the atoms must be well resolved, then the integral

$$a^2 \int_\alpha \rho(r+t)\rho^2(r)\,\mathrm{d}r \qquad (2)$$

will be small. Consequently, the difference between the two integrals, *i.e.* (1) − (2), should be a large positive value for the true structure. However, (2) becomes a large positive value for wrong $\rho(r)$ distributions containing poorly resolved peaks, *i.e.* peaks with widths greater than t. In these cases, the difference (1) − (2) will be smaller.

0108-7673/89/070490-05$03.00